

See discussions, stats, and author profiles for this publication at: <https://www.researchgate.net/publication/231665788>

# Enumeration and Evaluation of the Water Hexamer Cage Structure

ARTICLE *in* THE JOURNAL OF PHYSICAL CHEMISTRY A · JANUARY 2000

Impact Factor: 2.69 · DOI: 10.1021/jp992711t

---

CITATIONS

48

---

READS

12

3 AUTHORS, INCLUDING:



James V Coe

The Ohio State University

86 PUBLICATIONS 3,156 CITATIONS

SEE PROFILE

## Enumeration and Evaluation of the Water Hexamer Cage Structure

Michael D. Tissandier, Sherwin J. Singer, and James V. Coe\*

Department of Chemistry, The Ohio State University, 100 West 18th Avenue, Columbus, Ohio 43210-1173

Received: July 30, 1999; In Final Form: November 4, 1999

A topological enumeration has identified all hydrogen bond arrangements of the  $(\text{H}_2\text{O})_6$  cage, prism, book, chair, and boat frameworks. The 27 chemically distinct H-bond topologies of the cage structure were optimized for geometry and vibrationally analyzed with the PM3 semiempirical method. The structures, which differ only by the arrangement of the H-bonds, have minimized energies falling in a range of 10 kcal/mol and have dipole moments varying from 0 to 11 D. Stability of the structures is correlated with an increase in the number of single donor/single acceptor water (SD-SA) molecules. With structures of the same number of SD-SA water molecules, stability is anticorrelated with the dipole moment. The global minimum-energy structure has been identified and is one of four of particularly stable cage structures related by free hydrogen flipping. The lowest energy structures may interconnect as a result of large-amplitude quantum mechanical motion. The global minimum cage structure is also found to be more stable than the lowest energy, topologically enumerated structures of the prism, book, chair, and boat frameworks.

### Introduction

Cluster investigations employing approaches successful for small, gas-phase molecules face a daunting increase in complexity and difficulty as clusters grow in size. There is a need to develop systematic approaches to exploring the high dimensionality of cluster potential energy surfaces. Systematic numerical approaches to this problem include the “basin-hopping” method<sup>1</sup> used by Wales and Hodges,<sup>2</sup> diffusion equation method,<sup>3</sup> simulated annealing<sup>4,5</sup> shift method,<sup>6</sup> Gaussian density annealing,<sup>7</sup> the eigenmode method,<sup>8</sup> and the genetic algorithm.<sup>9,10</sup> Analytical guidance complementing the vast amount of numerical work on water clusters can be provided in graph theoretical treatments<sup>11–13</sup> as in the work of McDonald, Ojamäe, and Singer<sup>14</sup> on dodecahedral  $(\text{H}_2\text{O})_{20}$  and cube-shaped  $(\text{H}_2\text{O})_8$  frameworks. Their work was limited to waters with three-coordinate hydrogen bonding (H-bonding) and has been extended in this work to include waters with two-coordinate H-bonding. Since the most stable structures of  $(\text{H}_2\text{O})_{2–5}$  are now generally agreed to be cyclic, the  $(\text{H}_2\text{O})_6$  cluster is interesting as the smallest water cluster to favor more three-dimensional structures.<sup>15,16</sup> This work was started as a first step in applying these methods to larger clusters that are more directly related to known bulk ice structures. It is also hoped that these studies will focus the application of more sophisticated computational methods on some interesting aspects of the hexamer cage problem.

There has been much recent progress concerning the water hexamer cage structure. The cage framework consists of 4 central water molecules each participating in three H-bonds and 2 terminal waters each participating in two H-bonds. It was first given as a minimum-energy water hexamer structure in the work of Kim, Dupuis, Lie, and Clementi using Monte Carlo molecular dynamics techniques with the MCY potential.<sup>4</sup> Their cage structure constitutes one of “four nonequivalent but nearly degenerate cage structures” found to be the lowest energy  $(\text{H}_2\text{O})_6$  isomer by Wales (cited as a private communication in ref 15) as confirmed in this work. These four structures differ only by the arrangement of the “free” H atoms of the two terminal water

molecules, i.e., by hydrogen flipping. Saykally and co-workers<sup>15</sup> have impressively recorded high resolution, far-infrared vibration spectra of the water hexamer in cold supersonic jets. Their rotational constants appear to be most consistent with the cage framework, as opposed to prism, book, chair or boat frameworks. They note the compelling (though not definitive) argument that “no structures other than the most stable have ever been detected by VRT spectroscopy for any cluster in 6 K argon supersonic jets”. Ab initio work of Jordan and co-workers<sup>16,17</sup> finds several frameworks to be of comparable stability. The prism shows the most stable equilibrium structure, but the cage is found to be most stable after consideration of zero-point energies. The DQMC calculations with a model potential of Gregory and Clary<sup>15</sup> come to a similar conclusion. The TIP4P and MCY models,<sup>17</sup> as well as the presently used PM3 semiempirical method,<sup>18,19</sup> also find the cage to be most stable. Evidence is mounting for the cage as the most stable form of  $(\text{H}_2\text{O})_6$ .

Unlike previous numerical approaches to the enumeration of the isomers of  $(\text{H}_2\text{O})_6$ , in this work we employ a graph theoretical “topological enumeration” technique. This provides a framework for organizing the many possible local minima, and provides information that can be used to test the completeness of numerical searches. The steps needed to list all possible hydrogen bond structures for the  $(\text{H}_2\text{O})_6$  cage are explained in the following two sections.

### Enumeration of the H-Bond Topologies within the $(\text{H}_2\text{O})_6$ Cage

The topological enumeration of the water hexamer cage starts by labeling a cagelike framework of tetrahedrally oriented oxygens as given in Figure 1. The oxygens of the 4 central water molecules (each of which participates in 3 H-bonds) are labeled O1, O2, O3, and O4. The oxygens of the 2 terminal water molecules (each of which participates in 2 H-bonds) are labeled O5 and O6. The free H atoms, which in certain topologies dangle from oxygens O5 and O6, are not fixed by Bernal–Fowler ice rules. However, if we employ elementary

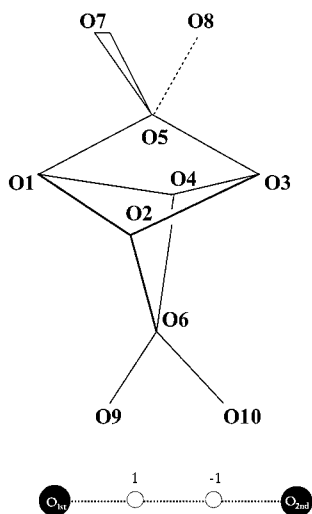


**Figure 1.** Hexamer cage framework with the oxygen positions labeled for the enumeration given in Table 1. Positions O1 through O4 have three-coordinate waters and positions O5 and O6 have terminal, two-coordinate waters. Positions O7, O8, O9, and O10 are unoccupied by oxygen, but are needed to account for the two possible orientations of free hydrogens in single donor–single acceptor (SD-SA) water molecules at the terminal positions. The bottom diagram demonstrates the numbering system used in Table 1.

notions of tetrahedral arrangement of acceptor and donor sites in the water molecule, the dangling H atoms from two-coordinate water molecules should point in one of two tetrahedral directions defined relative to the oxygen framework. Low-level electronic structure calculations are described later to check this assumption. In order to properly treat the arrangement of free H atoms from dangling two-coordinate waters, we introduce unoccupied oxygen positions to provide sites toward which the free H atoms are oriented. In the case of the hexamer cage, the terminal waters are two-coordinate and the unoccupied sites are labeled as O7, O8, O9, and O10. There are 12 possible H-bond positions to consider between the oxygen atoms in the 10 O atom framework of Figure 1. These framework connections are labeled by the oxygen atoms at each end of the connection, such as O2–O1 or O3–O1, and given as the column headings in Table 1. Even though they are drawn like bonds in Figure 1, each connection can harbor a H atom in either of two positions, O–H...O or O...H–O, as designated at the bottom of Figure 1. An entry of “1” under an oxygen framework connection heading in Table 1 indicates that the H atom is closest to the first oxygen as ordered in the heading, and an entry of “–1” indicates that the H atom is closest to the second oxygen. The last four columns differ by involving unoccupied oxygen positions. In these, an entry of “0” indicates no H atom and an unoccupied first oxygen position. The entries of “1”, “0”, or “–1” in the oxygen framework connections specify a structure. Considering that there are two choices for each oxygen framework connection there are  $2^{12} = 4096$  possible arrangements to consider at the outset. The chemical nature of a water’s hydrogen bonding and the topological symmetry of possible arrangements are used to reduce the possible arrangements or configurations down to only 27 chemically meaningful and chemically distinct structures.

The fact that each water can receive at most two H-bonds and donate at most two H-bonds is known as the Bernal–Fowler ice rules.<sup>20,21</sup> The ice rules can be posed in the present formulation in terms of Table 1 column entries as the following six quantities:  $q_1 = (\text{O2–O1}) + (\text{O4–O1}) + (\text{O5–O1})$ ,  $q_2 = (\text{O3–O2}) + (\text{O6–O2}) - (\text{O2–O1})$ ,  $q_3 = (\text{O4–O3}) + (\text{O5–}$

$\text{O3}) - (\text{O3–O2})$ ,  $q_4 = (\text{O6–O4}) - (\text{O4–O1}) - (\text{O4–O3})$ ,  $q_5 = 2(\text{O7–O5}) + 2(\text{O8–O5}) - (\text{O5–O1}) - (\text{O5–O3}) + 2$ , and  $q_6 = 2(\text{O9–O6}) + 2(\text{O10–O6}) - (\text{O6–O2}) - (\text{O6–O4}) + 2$ . To satisfy the ice rules,  $q_1$  through  $q_4$  must equal 1 or –1 and  $q_5$  and  $q_6$  must equal zero. After elimination of any arrangements that do not satisfy the ice rules, 194 structures remain.

Symmetry can also be applied to topological representations for structures (as opposed to actual molecular geometries) to identify identical configurations. The cage framework has  $D_{2d}$  symmetry. The group of permutations which preserve the connectivity of the oxygen framework induce a corresponding group on oxygen framework connections which are oriented by directional H-bonding. For example, the  $C_2$  operation, performed along an axis between O5 and O6, changes the oxygen framework connections as ordered in Table 1, i.e., {O2–O1, O4–O1, O5–O1, O3–O2, O6–O2, O4–O3, O5–O3, O6–O4, O7–O5, O8–O5, O9–O6, and O10–O6}, into {O4–O3, O2–O3, O5–O3, O1–O4, O6–O4, O2–O1, O5–O1, O6–O2, O8–O5, O7–O5, O10–O6, and O9–O6}, which could be written as {O4–O3, –(O3–O2), O5–O3, –(O4–O1), O6–O4, O2–O1, O5–O1, O6–O2, O8–O5, O7–O5, O10–O6, and O9–O6}. The latter notation emphasizes that H-bond topology is described by directional bonds. The mathematical entities used to capture this property are oriented graphs.<sup>11–13</sup> A particular set of entries for the oxygen framework connections, such as {1 1 –1 1 1 1 1 0 –1 0 0} (keeping the order of Table 1) becomes {1 –1 1 –1 1 1 –1 1 –1 0 0 0} under the  $C_2$  symmetry operation. This sequence can be checked against the original 194 ice-rule-allowed structures to see if it is the same as any others. If so, one of them is eliminated. After the topological application of  $D_{2d}$  symmetry operations, only 27 different configurations remained. The 27 different arrangements are given in Table 1.

## Structure Generation

Each topological arrangement in Table 1 was converted to an initial structure and optimized for geometry. The initial structures were based on a common O–O distance of 2.710 Å and an O–H bond length of 0.903 Å. All 27 structures were geometry-optimized with the semiempirical PM3 method<sup>18,19</sup> using the commercial programs Hyperchem 5.1<sup>22</sup> and Gaussian 94W.<sup>23</sup> Although ab initio methods are tractable for complexes as large as  $(\text{H}_2\text{O})_6$ , full geometry optimizations are computationally demanding because large basis sets are required to adequately describe H-bonded systems.<sup>24</sup> We employed the PM3 method as a practical means to sift through the large number of potential isomers for  $(\text{H}_2\text{O})_6$ . Ab initio treatments will be prohibitively costly for larger clusters, so it is worthwhile to gauge the effectiveness of semiempirical methods, which effectively include electron correlation and zero-point effects, for H-bonded systems.

There were a number of considerations in our choice of the PM3 semiempirical method. Unlike the MNDO and AM1 semiempirical methods, PM3 correctly predicts the linear H-bonded  $(\text{H}_2\text{O})_2$  structure as most stable (probably because water dimer is in the training set of molecules). PM3 also provides an approach for incorporating the flexibility of water molecules (unlike many frequently used water models). Zero-point energies are very important in evaluating the relative stabilities of water cluster structures. For example at  $n = 6$ , the prism structure has the most stable, equilibrium, ab initio structure; however, the cage becomes more stable upon consideration of zero-point energies.<sup>15,16</sup> High-level (MP4/aug-cc-pVDZ) calculations<sup>25</sup> of the equilibrium total association

**TABLE 1: Optimized Energy Relative to the Most Stable Structure, Dipole Moment, Number of Single Donor/Single Acceptor Waters (SD-SA), and Topological Designation for Each of the 27 Distinct Structures Associated with the Water Hexamer Cage Framework<sup>a</sup>**

struct	rel energy (kcal/mol)	dipole (D)	no. of SD-SA	topological designation for oxygen framework connections											
				O2-O1	O4-O1	O5-O1	O3-O2	O6-O2	O4-O3	O5-O3	O6-O4	O7-O5	O8-O5	O9-O6	O10-O6
1	0.00	1.72	2	1	1	-1	1	-1	1	1	1	0	-1	-1	0
2	0.02	1.61	2	1	1	-1	1	-1	1	1	1	-1	0	-1	0
3	0.04	1.72	2	1	1	-1	1	-1	1	1	1	0	-1	0	-1
4	0.15	1.96	2	1	1	-1	1	-1	1	1	1	-1	0	0	-1
5	0.76	2.87	2	1	1	-1	1	1	-1	1	-1	0	-1	0	-1
6	0.83	3.09	2	1	-1	1	1	1	1	-1	-1	0	-1	0	-1
7	1.43	4.43	2	1	1	-1	1	1	-1	1	-1	0	-1	-1	0
8	1.48	4.36	2	1	1	-1	1	1	-1	1	-1	-1	0	0	-1
9	1.64	4.58	2	1	-1	1	1	1	1	-1	-1	0	-1	-1	0
10	1.64	4.62	2	1	-1	1	1	1	1	-1	-1	-1	0	0	-1
11	2.23	5.63	2	1	1	-1	1	1	-1	1	-1	-1	0	-1	0
12	2.57	5.94	2	1	-1	1	1	1	1	-1	-1	-1	0	-1	0
13	2.61	4.65	1	1	1	-1	1	-1	-1	1	-1	-1	0	-1	-1
14	2.72	3.61	1	1	-1	1	1	-1	1	-1	-1	-1	0	-1	-1
15	2.99	3.69	1	1	-1	1	1	-1	1	-1	-1	0	-1	-1	-1
16	2.99	5.02	1	1	1	-1	1	1	-1	1	1	-1	0	0	0
17	3.01	3.63	1	1	-1	1	1	1	1	1	-1	0	0	-1	0
18	3.26	3.72	1	1	-1	1	1	1	1	1	-1	0	0	0	-1
19	3.74	4.55	1	1	1	-1	1	1	1	1	1	0	-1	0	0
20	3.82	5.68	1	1	1	-1	-1	1	-1	-1	-1	-1	-1	0	-1
21	4.25	5.63	1	1	1	-1	1	1	1	1	1	-1	0	0	0
22	4.40	6.39	1	1	1	-1	1	-1	1	-1	1	-1	-1	-1	0
23	4.51	0.00	0	1	-1	-1	1	-1	1	-1	-1	-1	-1	-1	-1
24	4.79	0.00	0	1	-1	1	1	1	1	1	1	0	0	0	0
25	4.95	6.42	0	1	-1	1	1	-1	1	1	-1	0	0	-1	-1
26	8.57	8.93	0	1	1	-1	1	1	1	-1	1	-1	-1	0	0
27	9.67	10.93	0	1	1	-1	-1	1	1	-1	1	-1	-1	0	0

<sup>a</sup> Structures have been numbered from most to least stable. The most stable structure (1) has a PM3 atomic binding energy of -1333.78 kcal/mol. In the oxygen framework columns a "1" designates a H near the first O and a "-1" designates a H near the second O. In the last four columns with unoccupied oxygens, a "0" means no H.

energies ( $n\text{H}_2\text{O} \rightarrow (\text{H}_2\text{O})_n$ ) of -4.36, -13.64, and -23.80 kcal/mol for  $n = 2, 3$ , and 4, respectively, change when corrected for zero-point energies to -2.23, -8.27, and -15.52 kcal/mol for  $n = 2, 3$ , and 4, respectively. One might also worry about thermal effects. For  $n = 2$ , the equilibrium MP2/AUG-cc-pVDZ binding energy corrects to a room temperature binding enthalpy of -3.2 kcal/mol.<sup>24</sup> Since the PM3 parameters are trained on experimental room temperature enthalpies of formation, they can incorporate thermal and zero-point energy effects albeit in a theoretically unsatisfying manner, i.e., in a nonseparable and system specific manner. The PM3 association energies are -3.50, -10.07, and -18.36 kcal/mol, for  $n = 2, 3$ , and 4, respectively. They fall between the ab initio equilibrium and zero point energy corrected results and are close to the thermally averaged (and zero point energy corrected) ab initio result at  $n = 2$ . This suggests that PM3 may furnish a rough guide to evaluating the energies of zero point structures of neutral water clusters at sizes prohibitively large for ab initio methods, particularly when many structures must be compared and considering that the ab initio methods require vibrational analysis.

## Results and Discussion

A local minimum of the PM3 potential energy surface was found for each of the 27 possible H-bond topologies of the  $(\text{H}_2\text{O})_6$  cage. Significantly, the two "tetrahedral" positions for the free H atoms of the two-coordinate waters led to distinct local minima, confirming the enumeration method described in the previous section. The structures are labeled and ordered by their PM3-optimized energies (relative to the most stable structure) in Table 1. Dipole moments are also tabulated. Different structures that happen to have nearly the same energy,

such as **15** and **16**, are clearly differentiated by the dipole moments. All 27 structures were vibrationally analyzed and all gave 48 real vibrational frequencies providing evidence for a real local minima in the PM3 potential surface for each topological structure. This does not mean that all 27 structures will be real minima on potential surfaces determined with higher levels of theory, but it does suggest that a complete search of the potential should involve these regions of the potential.

Ball and stick structures labeled by order of stability are given for all 27 distinct cage structures in Figure 2. Boxes define groups of structures related by hydrogen flipping of the free hydrogens on the terminal waters. The structures have also been grouped and characterized by the number of alternate free hydrogen flipping positions, i.e., single donor/single acceptor waters (SD-SA) as in Table 1 and by the large numbers on the right side of Figure 2. The optimized energies are plotted in Figure 3 and, even though each contains exactly 8 hydrogen bonds, their energies extend over a range of about 10 kcal/mol. Stability is correlated with an increase in the number of SD-SA water molecules. With structures of the same number of SD-SA water molecules, stability is anticorrelated with the dipole moment. A value of 1.85 D has been measured for the dipole moment component along the  $a$ -inertial axis of the cage hexamer.<sup>26</sup> Associated calculations<sup>26</sup> show this measurement to be consistent with a total dipole moment of 2.05 D. The total dipole moments of the four most stable structures fall within a range of 1.6–2.0 D which seems in reasonable agreement. Dipole moments of this size are not enough to bind electrons ( $\sim 2.5$  D);<sup>27</sup> however, there are 21 other structures with dipole moments falling in a range from 2.8 to 10.9 D that are large enough to bind electrons. When one states that the cage structure cannot bind electrons, these statements probably refer to



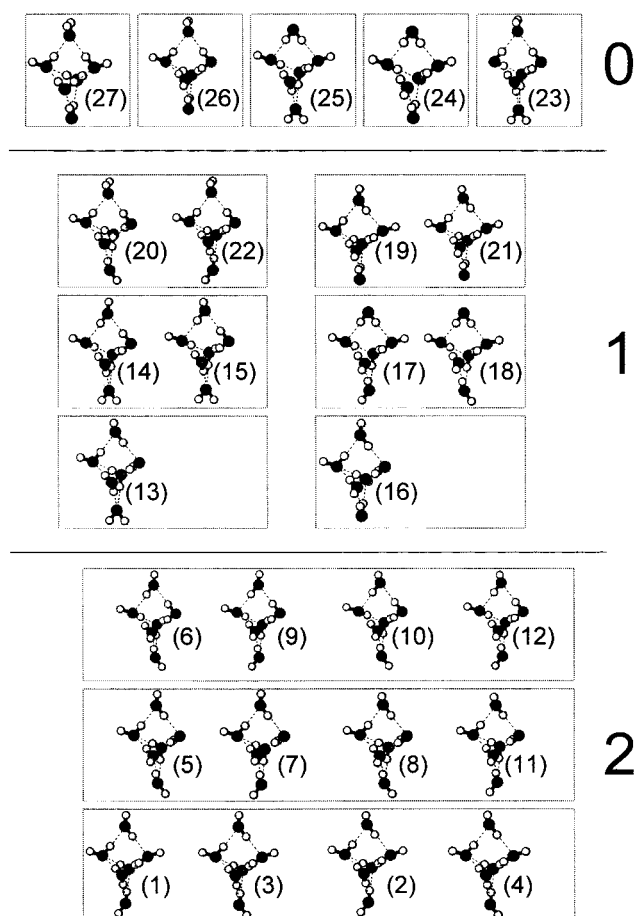


**Figure 2.** The 27 chemically distinct cage structures for the water hexamer. The large numbers along the right side designate how many single donor–single acceptor (SD-SA) positions are present in each structure. The individual structures are numbered according to their relative energies with **1** being most stable. The boxes contain related structures with identical frameworks which have similar, but not identical energies, due to H-flipping. The structures labeled **13** and **16** have only one such arrangement since the alternative free hydrogen orientation is equivalent by symmetry.

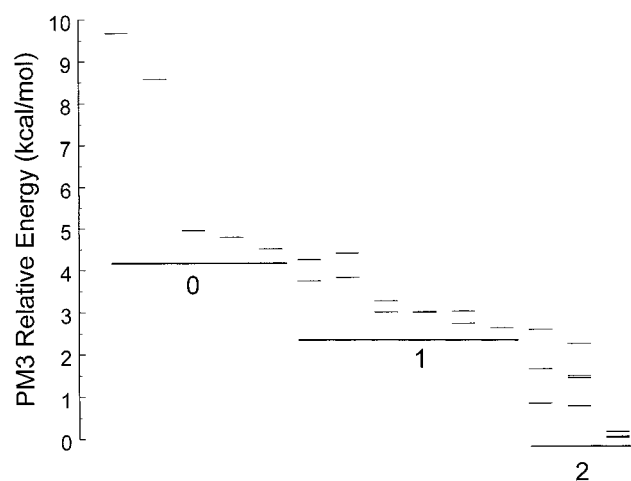


**Figure 3.** Relative energy of the cage structures arranged by the number of single donor–single acceptor (SD-SA) water molecules present. A general increase in stability is demonstrated to correlate to an increase in the number of SD-SA terminal waters present in the structure. H-flipping motions relate the vertically stacked energy levels.

structures **1–4** and also, technically, structures **23** and **24**. All of the rest are candidates for anionic systems with dipole-bound electrons.

The four most stable cage structures (each with two SD-SA waters related by hydrogen flipping) fall within a range 0.61 kcal/mol. The most stable structure has a PM3 atomic binding energy ( $6\text{O} + 12\text{H} \rightarrow (\text{H}_2\text{O})_6$ ) of  $-1333.78$  kcal/mol and is designated  $\{1\ 1\ -1\ 1\ -1\ 1\ 1\ 0\ -1\ 0\}$  or structure **1**. With a PM3 atomic binding energy of  $-217.222$  kcal/mol for a single water molecule, the excess molecular binding energy ( $6\text{H}_2\text{O} \rightarrow (\text{H}_2\text{O})_6$ ) is  $-30.45$  kcal/mol for the whole cluster or  $-5.07$  kcal/mol per water in the cluster. This is the same minimum found by Wales and Hodges<sup>2</sup> (their structure **6** with the TIP4P and ASP models) and Tsai and Jordan<sup>17</sup> (their structure **1** with TIP4P and rigid-water MP2/6-31+G\*\* intermolecular optimization). This structure is just a H-flip from structure **3** or  $\{1\ 1\ -1\ 1\ -1\ 1\ 1\ 0\ -1\ 0\ -1\}$  which is the minima presented by Clementi and co-workers<sup>4</sup> (their structure **6T**), Scheraga and co-worker's diffusion equation results<sup>3</sup> (their structure **6GL**), and Jordan and co-workers ab initio results<sup>16</sup> (their structure **I**). While structures **1–4** are very similar, they are not identical. Each has a unique energy, as well as a unique dipole moment. This stands in contrast to structures such as **13** and **16** whose H-flipping partners are equivalent by symmetry. To understand the fluxional nature of the hexamer cage, it will be important to compare and report the relative energies and barriers between the four lowest energy structures for various computational approaches that might be employed.

It is interesting to consider whether the four lowest minima of the  $(\text{H}_2\text{O})_6$  cage are accessible from each other either by quantum fluctuations in the ground state or by tunneling since low-energy barriers and hydrogen motion are involved. We constructed a potential surface for hydrogen flipping by adopting a pseudorotation coordinate for each of the free Hs on the terminal waters. The hydrogen flipping of the free H of O5 was defined by an improper dihedral angle ( $\varphi_1$ ) of the free H on O3, O3, O5, and the free H on O5. The hydrogen flipping of the free H of O6 was defined by an improper dihedral angle ( $\varphi_2$ ) of O3, O4, O6, and the free H on O6. These angles were constrained with artificially high force constants ( $3000$  kcal/mol/ $\text{\AA}^2$ ) which allowed the rest of the molecule to be optimized for fixed values of  $\varphi_1$  and  $\varphi_2$ . If these angles were normal coordinates, this procedure would reduce to generating the potential in these two normal coordinates. The potential surface,  $V(\varphi_1, \varphi_2)$ , generated in this fashion (see Figure 4) exhibits smaller barriers along the  $\varphi_2$  direction ( $\sim 0.7$  kcal/mol) than the  $\varphi_1$  direction ( $\sim 1.2$  kcal/mol). The four wells are inequivalent and the details of the inequivalency will be important in determining the nature of the splittings arising in such a potential.

Additional calculations suggest that large-amplitude motion of the free hydrogens of the  $(\text{H}_2\text{O})_6$  cage could possibly connect some or all of the four lowest energy isomers. There exist two PM3 normal vibrational modes which predominantly involve the free hydrogen flipping motion. They have harmonic frequencies of  $218$  and  $237\text{ cm}^{-1}$  that correspond to transitions reaching above the  $\varphi_1$  and  $\varphi_2$  barriers. The similarity of these normal coordinates to the  $\varphi_1$  and  $\varphi_2$  angles previously defined prompted an approximation of the motion of the free hydrogens as a hindered rotation of the terminal waters about their H-bonded O–H bond. The effective moment of inertia depends on the distance of the free hydrogen to the rotation axis. We employed the Colbert–Miller DVR method<sup>28</sup> to obtain the eigenvalues of the two-dimensional hindered rotor Hamiltonian

$$-\frac{\hbar^2}{2mR_{\text{eff}}^2} \left( \frac{\partial^2}{\partial \varphi_1^2} + \frac{\partial^2}{\partial \varphi_2^2} \right) + V(\varphi_1, \varphi_2) \quad (1)$$

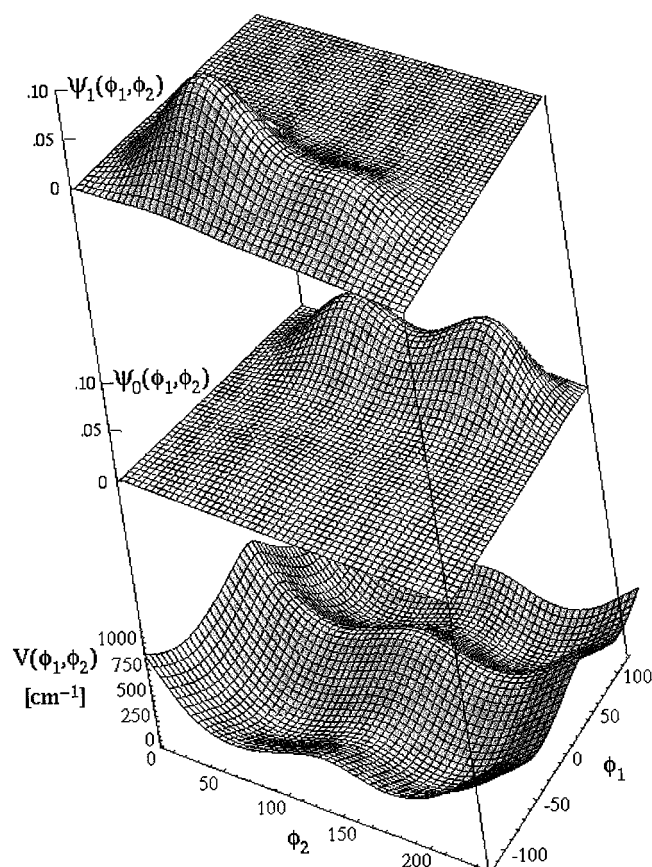


**Figure 4.** At the bottom is the potential energy surface,  $V(\varphi_1, \varphi_2)$ , in the two H-flipping coordinates of the terminal waters of the hexamer cage. The flipping of the free H of O5 is defined by an improper dihedral angle,  $\varphi_1$ , and the flipping of the free H of O6 is defined by an improper dihedral angle,  $\varphi_2$ . Each well corresponds to one of the four lowest energy cage structures (1–4). The calculated barrier heights differ and range from 0.5 to 1.5 kcal/mol. Wave functions for the two lowest energy states,  $\psi_0$  and  $\psi_1$  shown above the potential, were calculated with a hindered rotor Hamiltonian using  $m = 1$  amu and  $R_{\text{eff}} = 1.5$  bohr. They reveal delocalization among two of the four wells as the barrier in the  $\varphi_2$  coordinate is close to the zero-point energy.

using various values of  $R_{\text{eff}}$  and  $m$  equal to the proton mass. Representative results for the intermediate value of  $R_{\text{eff}} = 1.5a_0$ , shown in Figure 4, indicate delocalization among two of the four wells. We found that a small range of  $R_{\text{eff}}$  values near the physical projection of the free O–H bond onto the H-bonded O–H of the terminal waters could lead to highly disparate vibrational behavior. Small values of  $R_{\text{eff}}$  led to complete delocalization among the four wells of  $V(\varphi_1, \varphi_2)$ , while larger values forced complete localization in one well. Since barrier heights might be significantly different with better potential surfaces, we hope that this work will encourage a higher level approach to better predict the degree of quantum delocalization.

In addition to the cage framework, topological enumerations were also performed on the book, prism, chair, and boat frameworks. In accordance with experiment<sup>15</sup> and high-level ab initio calculations<sup>17,16</sup> corrected for zero-point energies, PM3 predicts the  $(\text{H}_2\text{O})_6$  cage structure to be the most stable isomer. This suggests that the PM3 method may be useful in approaching larger clusters. Whereas 27 distinct topological structures were found for the cage, 96, 10, 70, and 194 were found for the book, prism, chair, and boat, respectively. Unlike the case of the cage, not all of the distinct topologies correspond to stable geometrical structures or local minima on the PM3 potential surface. Some exhibit imaginary vibrational frequencies or

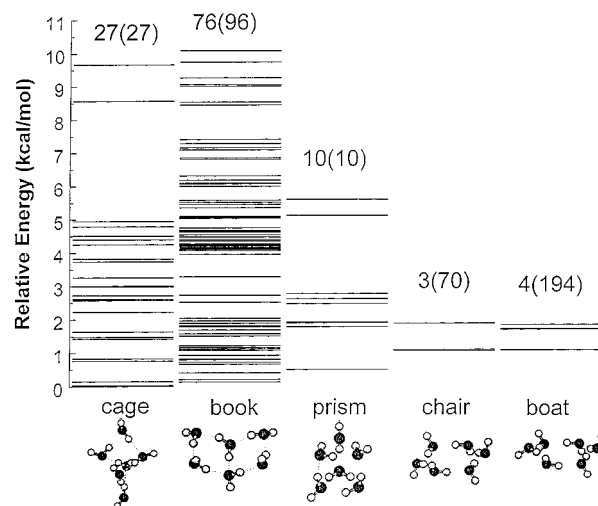


**Figure 5.** Relative PM3 energies of the four major hexamer frameworks. A ball and cylinder picture of the most stable structure for each framework is displayed. The large number at the top of each set of bars is the number of chemically distinct real minima. The corresponding number of topologically enumerated structures is given in parentheses. Not all topologies give rise to real minima. Some of the local minima, particularly less stable ones, may not be true minima on the potential surfaces of higher levels of theory.

collapse to other structures upon optimization, showing that they are not true minima. True local minima were found for 76 out of 96 book structures, 10 out of 10 prism structures, 3 out of 70 chair structures, and 4 out of 194 boat structures. The optimized energies of the various enumerated frameworks are presented in Figure 5. A total of 120 true local minima on the PM3 potential energy surface have been identified with the cage, book, prism, chair, and boat structures; however, there are other families of structures not presently considered (see structures 4, 22, 24, 28, 32, and 43 of ref 16). Tsai and Jordan<sup>17</sup> found 137 distinct minima with their eigenmode-following search procedure using a TIP4P potential. It would be very interesting to know how many of these could be classified as cage, book, prism, chair, or boat structures. The present work suggests that there should be, for instance, 27 cage and 10 prism structures. The present work can serve to calibrate the completeness of numerical search procedures. Although we have not undertaken the task, it would seem possible to use the present methods to determine a fairly complete tabulation of all of the local minima to be expected on the hexamer potential energy surface.

The semiempirical PM3 method finds the cage framework to have the most stable structure in agreement with the consensus emerging from other studies,<sup>15</sup> but there are book structures that fall within the range of the four most stable cage structures. There is only a 1.00 kcal/mol barrier<sup>22,29</sup> between the lowest energy book structure and cage structure (4), which are related by the formation of an extra H-bond between the upper right-hand side and lower left-hand side of the book as viewed in Figure 5. The cage structure (4) is probably accessible to the other lowest energy cage structures by tunneling or quantum fluctuations in the vibrational ground state. It would be very interesting to see this issue explored with a higher level method.

The order of stability of the most stable structure within a framework is cage > book > prism > chair, but the energies are within a range of about 1 kcal/mol. The enumerated structures of different frameworks vary within a range of  $\sim 10$  kcal/mol, so any arbitrarily chosen arrangement of H-bonds in these frameworks is likely to be considerably higher in energy than the lowest energy structure of each framework. It is also

**TABLE 2: Cartesian Coordinates in Standard Orientation, Equilibrium Rotational Constants, and Atomic Binding Energies of the PM3-Optimized Minimum-Energy Structures of the Most Stable Cage, Book, Prism, and Chair Frameworks**

atom	cage <sup>a</sup>			book <sup>b</sup>		
	X (Å)	Y (Å)	Z (Å)	X (Å)	Y (Å)	Z (Å)
O	0.67982	1.66847	0.22469	-0.01444	-1.40688	0.86698
H	1.54472	1.23557	0.26190	-0.82663	-1.49669	0.34972
H	0.80199	2.60883	0.28673	-0.12523	-1.87516	1.68772
O	-0.92115	-0.00176	1.65020	0.00588	1.34004	0.84909
H	-0.44806	0.77331	1.33150	0.08181	0.39642	1.02379
H	-1.76238	-0.05171	1.18135	0.79287	1.61382	0.36582
O	0.63241	-1.64984	0.20904	2.39229	-1.33294	-0.43486
H	0.08923	-1.22268	0.89198	1.59349	-1.47091	0.08523
H	0.53282	-2.59214	0.27953	2.24183	-1.68508	-1.30567
O	-0.42478	0.02956	-1.62376	2.39226	1.39375	-0.42232
H	-0.09616	0.81284	-1.17004	2.55075	0.44513	-0.49263
H	0.00023	-0.73782	-1.22438	3.12911	1.78535	0.03323
O	2.74478	-0.02765	-0.08537	-2.40639	-1.30367	-0.41807
H	2.20281	-0.78880	0.15326	-2.58996	-0.35940	-0.32660
H	2.94467	-0.09143	-1.01363	-2.41112	-1.51135	-1.34633
O	-2.76330	-0.07803	-0.30968	-2.36824	1.39716	-0.44640
H	-2.08455	-0.14812	-0.99436	-1.47660	1.53891	-0.10056
H	-3.30763	-0.76710	-0.50478	-2.97126	1.91930	0.07093

atom	prism <sup>c</sup>			chair <sup>d</sup>		
	X (Å)	Y (Å)	Z (Å)	X (Å)	Y (Å)	Z (Å)
O	1.38240	-0.79588	1.21410	-2.61489	-0.49801	-0.05964
H	0.45622	-0.77606	1.50601	-2.18720	-0.16571	0.73755
H	1.91210	-1.20090	1.89061	-2.84109	-1.40951	0.09263
O	1.48104	1.37700	-0.30523	-1.30567	-0.05649	-2.42030
H	1.66217	0.81313	0.45827	-1.71801	-0.27675	-1.57725
H	2.14568	2.05442	-0.35742	-1.77602	0.68145	-2.79269
O	1.06670	-1.01572	-1.39720	1.41891	0.07745	-2.34081
H	1.28587	-1.35829	-0.52354	0.45743	0.14256	-2.32623
H	1.27925	-0.07519	-1.39115	1.65236	-0.68557	-2.85838
O	-1.27339	-0.50500	1.53311	2.61489	0.49801	0.05964
H	-1.33645	0.44562	1.36259	2.18720	0.16571	-0.73755
H	-1.58576	-0.94802	0.73654	2.84109	1.40951	-0.09263
O	-1.20461	1.67808	0.04663	1.30567	0.05649	2.42030
H	-0.27064	1.81552	-0.13712	1.71801	0.27675	1.57725
H	-1.54482	1.05338	-0.60204	1.77602	-0.68145	2.79269
O	-1.58571	-0.71089	-1.07832	-1.41891	-0.07745	2.34081
H	-0.70068	-0.95230	-1.38904	-0.45743	-0.14256	2.32623
H	-2.23434	-1.09209	-1.65835	-1.65236	0.68557	2.85838

<sup>a</sup> Rotational constants (GHz): 2.4522, 1.2419, 1.2137; ABE = -1333.78 kcal/mol. <sup>b</sup> Rotational constants (GHz): 2.0431, 1.1034, 0.8173; ABE = -1333.57 kcal/mol. <sup>c</sup> Rotational constants (GHz): 1.9532, 1.5377, 1.5255; ABE = -1333.19 kcal/mol. <sup>d</sup> Rotational constants (GHz): 1.2756, 1.2062, 0.6307; ABE = -1332.81 kcal/mol.

notable that the dipole moments of less stable structures can be very different than those of the most stable structures. The Cartesian coordinates of the most stable structures are provided for each of the frameworks in Table 2 as a starting step to facilitate higher level approaches.

In conclusion, a method has been presented by which one can be sure that all candidate structures for a chosen framework have been evaluated. Twenty-seven distinct structures are reported for the water hexamer cage framework. The most stable cage structure has also been found to be a global minimum with regard to the book, prism, boat, and chair frameworks within the PM3 model. The completeness of the approach is particularly noteworthy. While the entropic contributions associated with

supposedly near-degenerate arrangements of hydrogen bonds in ice Ih are well-known,<sup>30</sup> we were surprised to find such large enthalpic variations with the arrangement of hydrogen bonds in hexamer frameworks. The present method is currently being extended to significantly larger water clusters in an effort to connect with bulk icelike cubic and hexagonal structures. It is hoped that studies such as this will provide guidance and evaluation to the various numerical procedures that search for global minima on the rugged landscapes of water cluster potential energy surfaces.

**Acknowledgment.** J.C. and M.T. thank the NSF (CHE-9528977).

## References and Notes

- (1) Li, Z.; Scheraga, H. A. *Proc. Natl. Acad. Sci. U.S.A.* **1987**, *84*, 6611.
- (2) Wales, D. J.; Hodges, M.; P. *Chem. Phys. Lett.* **1998**, *286*, 65–72.
- (3) Wawak, R. J.; Wimmer, M. M.; Scheraga, H. A. *J. Phys. Chem.* **1992**, *96*, 5138–5145.
- (4) Kim, K. S.; Dupuis, M.; Lie, G. C.; Clementi, E. *Chem. Phys. Lett.* **1986**, *131*, 451–6.
- (5) Lee, C.; Chen, H.; Fitzgerald, G. J. *Chem. Phys.* **1995**, *102*, 1266–9.
- (6) Pillardy, J.; Olszewski, K. A.; Piela, L. *J. Mol. Struct. (THEOCHEM)* **1992**, *270*, 277–85.
- (7) Tsao, C.; Brooks, C. L. *J. Chem. Phys.* **1994**, *101*, 6405–35.
- (8) Tsai, C. J.; Jordan, K. D. *J. Phys. Chem.* **1993**, *97*, 11227–11237.
- (9) Jorgensen, W. L.; Chandrasekhar, J.; Madura, J. D.; Impey, R. W.; Klein, M. L. *J. Chem. Phys.* **1983**, *79*, 926–35.
- (10) Niesse, J. A.; Mayne, H. R. *J. Comput. Chem.* **1997**, *18*, 1233–44.
- (11) Radhakrishnan, T. P.; Herndon, W. C. *J. Phys. Chem.* **1991**, *95*, 10609–10617.
- (12) Harary, F.; Palmer, E. *Can. J. Math.* **1966**, *18*, 853.
- (13) Harary, F.; Palmer, E. *Bull. Acad. Polon. Sci. Ser. Sci. Math. Astronom. Phys.* **1966**, *14*, 125.
- (14) McDonald, S.; Ojamäe, L.; Singer, S. J. *J. Phys. Chem. A* **1998**, *102*, 2824–2832.
- (15) Liu, K.; Brown, M. G.; Carter, C.; Saykally, R. J.; Gregory, J. K.; Clary, D. C. *Nature (London)* **1996**, *381*, 501–503.
- (16) Kim, K.; Jordan, K. D.; Zwier, T. S. *J. Am. Chem. Soc.* **1994**, *116*, 11568–9.
- (17) Tsai, C. J.; Jordan, K. D. *Chem. Phys. Lett.* **1993**, *213*, 181–188.
- (18) Stewart, J. J. P. *J. Comput. Chem.* **1989**, *10*, 209–20.
- (19) Stewart, J. J. P. *J. Comput. Chem.* **1989**, *10*, 221–64.
- (20) Fletcher, N. H. *The Chemical Physics of Ice*; Cambridge: New York, 1970.
- (21) Hobbs, P. V. *Ice Physics*; Oxford: New York, 1974.
- (22) Hyperchem; 5.0 ed.; Hypercube, Inc., 1997.
- (23) Frisch, M. J.; Trucks, G. W.; Schlegel, H. B.; Gill, P. M. W.; Johnson, B. G.; Robb, M. A.; Cheeseman, J. R.; Keith, T.; Petersson, G. A.; Montgomery, J. A.; Raghavachari, K.; Al-Laham, M. A.; Zakrzewski, V. G.; Ortiz, J. V.; Foresman, J. B.; Peng, C. Y.; Ayala, P. Y.; Chen, W.; Wong, M. W.; Andres, J. L.; Replogle, E. S.; Gomperts, R.; Martin, R. L.; Fox, D. J.; Binkley, J. S.; Defrees, D. J.; Baker, J.; Stewart, J. P.; Head-Gordon, M.; Gonzalez, C.; Pople, J. A. *Gaussian 94*, Revision B.2; Gaussian, Inc.: Pittsburgh, PA, 1995.
- (24) Del Bene, J. E.; Shavitt, I. The quest for reliability in calculated properties of hydrogen-bonded complexes. In *Molecular Interactions*; Scheiner, S., Ed.; Wiley: Chichester, UK, 1997; pp 157–179.
- (25) Xantheas, S. S.; Dunning, T. H., Jr. *J. Chem. Phys.* **1993**, *99*, 8774–92.
- (26) Gregory, J. K.; Clary, D. C.; Liu, K.; Brown, M. G.; Saykally, R. J. *Science (Washington, DC)* **1997**, *275*, 814–817.
- (27) Hendricks, J. H.; de Clercq, H. L.; Lyapunova, S. A.; Bowen, K. H., Jr. *J. Chem. Phys.* **1997**, *107*, 2962–2967.
- (28) Colbert, D. T.; Miller, W. H. *J. Chem. Phys.* **1992**, *96*, 1982–1991.
- (29) Baker, J. *J. Comput. Chem.* **1986**, *7*, 385–395.
- (30) Eisenberg, D.; Kauzmann, W. *The Structure and Properties of Water*; Oxford University Press: New York, 1969.